Available online at www.sciencedirect.com
ScienceDirect
International Journal of Heat and Mass Transfer 50 (2007) 908–918
International Journal of HEAT and MASS TRANSFER
www.elsevier.com/locate/ijhmt

A dominant geometrical parameter affecting the turbulent mixing rate in rod bundles

Hae-Yong Jeong *, Kwi-Seok Ha, Young-Min Kwon, Yong-Bum Lee, Dohee Hahn

Fluid Engineering Division, Korea Atomic Energy Research Institute, 150 Deokjin-dong, Yuseong-gu, Daejeon 305-353, Republic of Korea

Received 10 February 2006; received in revised form 2 August 2006
Available online 25 October 2006

Abstract

The trends of turbulent mixing data in rod arrays and various definitions of the mixing factors are examined to derive a new definition of a mixing factor. The proposed mixing factor is based on the eddy diffusivity of energy and it takes into account the degree of the turbulent mixing of various fluids having different Prandtl numbers. With this definition of a mixing factor it is found that the geometrical parameter δ_{ij}/D_h is a dominant factor affecting a turbulent mixing, which correlates well with the reliable experimental data selected by considering the reliability of the measurement technique used in the experiments. A useful correlation of the turbulent mixing in rod arrays was developed as a function of δ_{ij}/D_h. The correlation is applicable for both square and triangular arrays with a reasonable accuracy. It predicts a reasonable mixing at a higher δ_{ij}/D_h or at a lower S/d ratio, which is the most improved feature of the correlation when compared with the existing ones. The proposed correlation may be applicable for the thermal-hydraulic design of a nuclear reactor with an improved accuracy.

Keywords: Subchannel analysis; Turbulent mixing; Mixing factor; Mixing coefficient; Rod bundle; Gap-to-diameter ratio; Geometrical parameter

1. Introduction

In the design of a nuclear reactor, it is very important to predict the detailed flow and temperature distributions in a reactor core. This is because a safe and reliable operation of a reactor system relies on an accurate thermal-hydraulic design. To calculate these distributions, the subchannel approach is frequently used. In a subchannel approach, the temperature, pressure and velocity in a subchannel is averaged, and one representative thermal-hydraulic condition specifies the state of the subchannel. To obtain the flow and temperature distributions with a subchannel analysis code, the conservations of the mass, momentum, and energy in a subchannel are modeled and solved. Therefore, it is required to model the inter-subchannel mixing phenomenon due to the cross flow between the adjacent subchannels as accurately as possible to enhance the predictability of a subchannel analysis code. Fig. 1 depicts the schematics of rod bundles and the subchannels where the inter-subchannel mixing occurs.

When a single-phase flow exists in the subchannels, a mixing of the mass, energy and momentum between the subchannels consists of two parts, a forced mixing and a natural one. The natural mixing again consists of a diversion flow and a turbulent mixing. The diversion flow mixing is mainly caused by the pressure gradient due to flow obstacles such as spacers or due to a density difference. The diversion flow is modeled appropriately with the distributed resistance model [1,2] and the axial pressure drop correlations [3,4].

The turbulent mixing, caused by the eddy motion of the fluid across the gap between the subchannels, enhances the exchange of the momentum and the energy through the gap with no net transport of the mass. In the subchannel analysis codes such as COBRA-IV [5] and MATRA-LMR-FB [6], the effects of a turbulent mixing are taken

* Corresponding author. Tel.: +82 42 868 8987; fax: +82 42 868 2075.
E-mail address: hyjeong@kaeri.re.kr (H.-Y. Jeong).

0017-9310/$ - see front matter © 2006 Elsevier Ltd. All rights reserved.
doi:10.1016/j.ijheatmasstransfer.2006.08.023

Nomenclature

A	subchannel flow area
B	constant in Eq. (34)
c	constant in Eq. (8)
c_p	specific heat at constant pressure
d	rod diameter
D	diffusion coefficient
D_h	hydraulic diameter of a subchannel
f	friction factor
f_T	turbulent momentum factor
g	gravitational constant
G	axial mass flux
$\overline{G}$	average axial mass flux
h	enthalpy
h^*	enthalpy from donor cell
k	thermal conductivity
K	form loss coefficient, constant in Eq. (30)
m	axial flow rate
n	normal direction
p	pressure
P	rod pitch
Pe_t	turbulent Peclet number, $(\varepsilon_M/\nu)Pr$
Pr	Prandtl number, $c_p\mu/k$
Pr_t	turbulent Prandtl number, $\varepsilon_M/\varepsilon_H$
q	heat
Q	heat input per unit length of the flow channel
Re	Reynolds number, $\rho u D_h/\mu$
S	gap size
Sc	Schmidt number, $\mu/(\rho D)$
St_g	gap Stanton number, $w'_{ij}/(S_{ij}G_i)$
T	temperature
u	axial velocity
u_τ	shear velocity
u'	fluctuating component of axial velocity
u^*	axial velocity from donor cell
$\bar{u}$	average axial velocity
v	transverse velocity
v_{eff}	effective mean mixing velocity
w	lateral flow rate
w'	fluctuating lateral flow rate
w_{ij}	lateral flow rate from subchannel i to j
x	coordinate of axial direction
Y	turbulent mixing factor
Y^*	Re-independent turbulent mixing factor
z	effective mixing length

Greek symbols

β	turbulent mixing coefficient
δ	distance between the center of two adjacent subchannels
Δ	node size
ε_H	eddy diffusivity for energy
ε_M	eddy diffusivity for momentum
$\bar{\varepsilon}$	reference eddy viscosity
ν	kinematic viscosity
ρ	density
μ	molecular viscosity

Subscripts

A	area-averaged
H	enthalpy or energy
i	subchannel i
ij	from subchannel i to j, between the subchannel i and j
j	subchannel j
S	gap averaged

into account in the axial momentum equation and the energy conservation equation. The axial momentum equation and the energy equation for an arbitrary subchannel i are described as follows, respectively:

$$\frac{\partial m_i}{\partial t}+\frac{\partial}{\partial x}\left(\frac{m_i^2}{\rho A_i}\right)+\sum_j w_{ij}u^*+\sum_j f_T(w'_{ij}u'_i-w'_{ji}u'_j) = -A\frac{\partial p}{\partial x}-A\rho g-\frac{1}{2}\left(\frac{f}{D_h}+\frac{K}{\Delta x}\right)\langle\rho u^2\rangle_A A, \quad (1)$$

$$A_i\frac{\partial}{\partial t}(\rho_i h_i)+\frac{\partial}{\partial x}(m_i h_i)+\sum_j w_{ij}h^*+\sum_j(w'_{ij}h_i-w'_{ji}h_j)=Q, \quad (2)$$

where Q denotes the heat input per unit length of the flow channel. These equations clearly suggest the importance of the modeling of a turbulent mixing in subchannel approaches.

In the above equations, the last terms in the left-hand sides represent the contribution by the turbulent mixing between subchannel i and its surrounding subchannels. Therefore, the turbulent mixing model in a subchannel code determines the turbulent mixing flow rate, w' and the turbulent momentum factor, f_T. The turbulent momentum factor is the same as the turbulent Prandtl number. The turbulent mixing flow rate from subchannel i to j per unit length is defined with the effective mean fluctuating velocity, v_{eff} as follows:

$$w'_{ij}\equiv\rho_i v_{eff}S_{ij}. \quad (3)$$

There are several methods to evaluate the turbulent mixing flow rate. Some researchers have calculated the turbulent mixing coefficients from the measured subchannel temperature and a computer simulation. The chemical tracer method, the hot-wire anemometry, and the laser Doppler anemometry are other possible experimental techniques. However, each method has one or more limitations in an application to a rod bundle geometry and considerable caution is required to obtain accurate data by using these

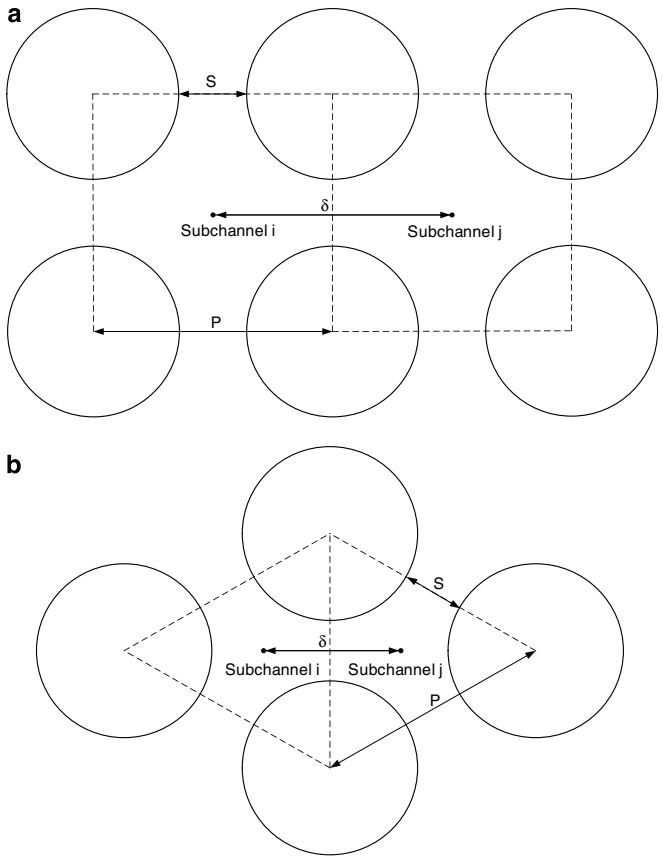

Fig. 1. Schematic diagram of rod bundle and flow channels. (a) Square array and (b) triangular array.

methods. Therefore, the data for rod bundles is not enough to develop a reliable correlation. Although some correlations have been developed for use in rod bundles, they show a rather large discrepancy with each other. This is mainly due to a scattering of the turbulent mixing data itself, used for the derivation of the correlations. In the present study, the reasons for the data scattering are studied and we attempt to suggest a more reliable correlation based on the existing data of a turbulent mixing.

2. Review of existing turbulent mixing data

When there is no diversion flow or forced mixing flow, the energy transport across a gap between the subchannels per unit length in rod bundles is equivalent to

$$q_{ij} = (k + \rho c_p \varepsilon_H) S_{ij} \left(\frac{\partial T}{\partial n}\right)_S \tag{4}$$

or

$$q_{ij} = k\left(1 + Pr\frac{\varepsilon_H}{\nu}\right) S_{ij} \left(\frac{\partial T}{\partial n}\right)_S . \tag{5}$$

The equations above mean that the energy transfer occurs due to heat conduction through the coolant itself and to turbulent eddy motion of the fluid. At the typical operating condition of a pressurized water reactor (PWR), the second term in the first bracket of Eq. (5) is of the order of 10^3. Therefore, the heat transfer by conduction is negligible in the design of a PWR. On the contrary, the order of the same quantity for a liquid metal-cooled reactor (LMR) is about $10^{-1} \sim 10^0$, which implies that both a heat conduction and a turbulent mixing play an important role in the thermal-hydraulics of an LMR.

In a subchannel approach, the conduction heat transfer is usually modeled by a simple conduction equation with a conduction shape factor, which is the ratio of the effective heat transfer distance to the centroid distance between subchannels [7]. The rate of turbulent mixing in rod bundles has not been predicted well with a conventional turbulent diffusion theory. Many experimental results in rod bundles have obtained much higher turbulent mixing rates than those predicted by the theory for a simple geometry. These experimental results imply that the eddy diffusivity of energy, ε_H for rod bundles is much higher than that obtained in a circular tube. Some researchers tried to explain this high turbulent mixing rate by the effect of the secondary flow formed in the subchannels. However, the analysis of turbulent structures in rod arrays by Rehme [8] has suggested that the main cause of a high mixing rate in compact rod bundles is due to a cyclic and periodic flow pulsation, which is usually referred to as the anisotropic turbulent motion. Therefore, several researchers have concentrated their efforts on developing a useful correlation by taking into account the anisotropic component of turbulence in rod bundles.

2.1. Turbulent mixing coefficient

The existing correlations on a turbulent mixing in rod bundles have been developed with different definitions of the mixing parameters. The most general form of a correlation is the turbulent mixing coefficient, β, defined by the ratio of the effective mean mixing velocity to the axial velocity as follows:

$$\beta = \frac{v_{\text{eff}}}{\bar{u}}. \tag{6}$$

This mixing coefficient is essentially the same as the gap Stanton number, St_g. This definition of a mixing coefficient was used in the correlations suggested by Row and Angle [9], Castellana [10], Seale [11], Cheng and Todreas [12]. The turbulent mixing coefficient is normally determined from the thermal mixing test for single-phase conditions. With this definition of a turbulent mixing coefficient, the turbulent mixing flow rate from channels i to j is

$$w'_{ij} = \beta S_{ij} \overline{G}_{ij}, \tag{7}$$

where $\overline{G}_{ij}$ is the average axial mass flux flowing along subchannels i and j. Some researchers such as Ramm [13], Rogers and Tahir [14] have suggested correlations with the mixing flow rate divided by the dynamic viscosity, which are easily converted to a correlation with the mixing coefficient, β per the relation of Eq. (7).

Recently, Cheng and Tak [15] performed a computational fluid dynamics (CFD) analysis for thermal-hydraulic behavior of lead–bismuth eutectic in subchannels of both triangular and square lattices. They calculated the velocity fluctuation across the gap and evaluated the turbulent mixing coefficient defined by Eq. (6). By normalizing the velocity fluctuation for the shear velocity and by adopting the Blasius equation for the evaluation of the shear friction, their results are expressed with the following equation:

$$\beta = \frac{cu_\tau}{\bar{u}} = 0.2cRe^{-0.125}. \tag{8}$$

Cheng and Tak also found that the coefficient c depends mainly on subchannel geometry and increases slightly with increasing Reynolds number. For the triangular lattice having the gap-to-diameter ratio S/d of 0.5, it was found that the mixing coefficient is about 0.02. The accuracy of the mixing coefficient evaluated by CFD calculation is still questionable because the degree of anisotropic turbulence is determined by the turbulence model incorporated in a CFD code.

In Table 1, some experimentally-determined correlations of the mixing flow rate or the turbulent mixing coefficient β are summarized. The correlations of the mixing flow rate are converted to the form of the turbulent mixing coefficient which is summarized in Table 2. The same correlations are also compared with each other in Fig. 2. The data shows considerable scattered characteristics because the geometry and the range of the Reynolds number for each experiment differ considerably. Actually, this was the main reason for the difficulty that many previous researchers encountered in obtaining a generalized correlation for the turbulent mixing factors. Therefore, the applicable range of most existing correlations is limited to a certain range of the Reynolds number and to the specified geometries.

Fig. 2 evidently indicates that a turbulent mixing decreases as the gap-to-diameter ratio S/d increases. Further, it is found that a turbulent mixing is generally reduced with an increase of the Reynolds number even though the effect of the Reynolds number diminishes at a higher Reynolds number especially with a large gap-to-diameter ratio. However, this trend is not trivial at a lower Reynolds number. In the figure, the turbulent mixing Stanton number obtained by Kelly and Todreas [16] in triangular rod arrays decreases as the Reynolds number decreases to lower than 8000 where the effect of a laminarization appears. The results by Galbraith and Knudsen [17] also show the laminarization effect as the Reynolds number decreases in square rod arrays. Petrunik [18], Singh and Pierre [19] also reported the decrease of the mixing coefficient with the decrease of the Reynolds number for a very small rod spacing. As described by Galbraith and Knudsen, there is a possibility that the turbulence transport mechanisms could be affected by the laminar sub-layer at a lower gap-to-diameter ratio, particularly at a lower Reynolds number. Singh and Pierre [19] mentioned that the data showing

Table 1
Summary of the major parameters for the mixing factor derived or used by researchers

Experimenter	S/d	Friction factor	Eddy diffusivity	w'_{ij}/μ	St_g or β	Y_H
Rowe and Angle [9]	0.036	$f = a \cdot Re^b$	$\varepsilon_H/\nu = 0.0062 \cdot Re^{0.9}$	–	$0.063 \cdot Re^{-0.1}$	$\left(\frac{\delta_{ij}}{D_h}\right) \cdot (\bar{\varepsilon}_M/\nu)^{-1} Re \cdot \beta \cdot Pr_t$
	0.149				$0.021 \cdot Re^{-0.1}$	
Castellana [10]	0.334	$f = a \cdot Re^b$	$\varepsilon_H/\nu \propto Re\sqrt{f/8}$	–	$0.027 \cdot Re^{-0.1}$	$\left(\frac{\delta_{ij}}{D_h}\right) \cdot (\bar{\varepsilon}_M/\nu)^{-1} Re \cdot \beta \cdot Pr_t$
Seale [11]	0.100	$f' = 0.053 \cdot Re^{-0.211}$	$\varepsilon_M/\nu = 0.00755 \cdot Re^{0.911}$	–	$0.02968 \cdot Re^{-0.1}$	$\left(\frac{\delta_{ij}}{D_h}\right) \cdot (\bar{\varepsilon}_M/\nu)^{-1} Re \cdot \beta \cdot Pr_t$
	0.375	[Hussain and Reynolds]			$0.01683 \cdot Re^{-0.1}$	
	0.833				$0.009225 \cdot Re^{-0.1}$	
Rogers and Rosehart [30]	–	–	–	–	$0.004 \cdot \left(\frac{D_h}{S}\right) Re^{-0.1}$	$\left(\frac{\delta_{ij}}{D_h}\right) \cdot (\bar{\varepsilon}_M/\nu)^{-1} Re \cdot \beta \cdot Pr_t$
Rogers and Tahir [14]	–	–	–	$0.0050 \cdot \left(\frac{S}{d}\right)^{0.106} Re^{0.9}$	$\left(\frac{w'}{\mu}\right) \cdot \left(\frac{D_h}{S}\right) Re^{-1}$	$\left(\frac{\delta_{ij}}{S}\right) \cdot (\bar{\varepsilon}_M/\nu)^{-1} \cdot \left(\frac{w'_{ij}}{\mu}\right) \cdot Pr_t$
	0.400	$f' = 0.044 \cdot Re^{-0.194}$		$0.0018 \cdot \left(\frac{S}{d}\right)^{-0.4} Re^{0.9}$		
Gabraith and Knudsen [17]	0.011	–	–	$7.5 \times 10^{-15} \cdot Re^{3.43}$	$\left(\frac{w'}{\mu}\right) \cdot \left(\frac{D_h}{S}\right) Re^{-1}$	$\left(\frac{\delta_{ij}}{S}\right) \cdot (\bar{\varepsilon}_M/\nu)^{-1} \cdot \left(\frac{w'_{ij}}{\mu}\right) \cdot Pr_t$
	0.028			$0.0001 \cdot Re^{1.23}$		
	0.063			$0.00037 \cdot Re^{1.12}$		
	0.127			$0.00050 \cdot Re^{1.12}$		
	0.228			$0.00190 \cdot Re^{1.01}$		
Kelly and Todreas [16]	0.100	$f' = 0.0780 \cdot Re^{-0.228}$ [cf. Blasius eq.]	$\varepsilon_H/\nu = 0.0045 \cdot Re^{0.89}$	$0.0021 \cdot Re^{0.935}$ [$8000 < Re < 24{,}000$]	$\left(\frac{w'}{\mu}\right) \cdot \left(\frac{D_h}{S}\right) Re^{-1}$	$\left(\frac{\delta_{ij}}{S}\right) \cdot (\bar{\varepsilon}_M/\nu)^{-1} \cdot \left(\frac{w'_{ij}}{\mu}\right) \cdot Pr_t$
Rehme [8]	–	$f = 0.18 \cdot Re^{-0.2}$	$\bar{\varepsilon}_M/\nu = 0.0075 \cdot Re^{0.9}$	–	–	–

Table 2
Dependency of turbulent mixing factor on Re shown in the previous studies

Experimenter	Channel type/ fluid	S/d	D_h (mm)	δ_{ij}/D_h	St_g or β	B	Pr_t	Y^*	Y_H^*
Rowe and Angle [9]	S-T/water	0.036	5.105	2.488	$0.063 \cdot Re^{-0.1}$	0.063	0.853	20.675	17.636
		0.149	7.290	1.769	$0.021 \cdot Re^{-0.1}$	0.021	0.853	4.901	4.180
Castellana [10]	S-S/water	0.334	13.56	1.054	$0.027 \cdot Re^{-0.1}$	0.027	0.851	3.754	3.195
Seale [11]	S-S/air	0.100	27.1	1.7176	$0.02968 \cdot Re^{-0.1}$	0.02968	0.856	6.725	5.757
		0.375	57.3	0.9296	$0.01683 \cdot Re^{-0.1}$	0.01683	0.855	2.064	1.765
		0.833	125.0	0.5710	$0.009225 \cdot Re^{-0.1}$	0.009225	0.855	0.695	0.591
Rogers and Rosehart [30]	S-S	–	–	–	$0.004 \cdot \left(\frac{D_h}{S}\right) Re^{-0.1}$	–	–	–	–
Galbraith and Knudsen [17]	S-S/water	0.011	10.57	2.6442	$2.8365 \times 10^{-13} \cdot Re^{2.43}$	–	–	–	–
		0.028	11.17	2.5011	$0.001571 \cdot Re^{0.23}$				
		0.063	12.42	2.2504	$0.002871 \cdot Re^{0.12}$				
		0.127	14.69	1.9018	$0.002277 \cdot Re^{0.12}$				
		0.228	18.29	1.5280	$0.005999 \cdot Re^{0.01}$				
Rogers and Tahir [14]	S-S	–	–	–	$0.005 \cdot \left(\frac{D_h}{S}\right) \cdot \left(\frac{S}{d}\right)^{0.106} \cdot Re^{-0.1}$	–	–	–	–
	T-T/air	0.400	29.4	0.699	$0.007479 \cdot Re^{-0.1}$	0.007479	0.866	0.644–0.829	0.565–0.709
Kelly and Todreas [16]	T-T/water	0.100	12.733	1.9000	$0.0070 \cdot Re^{-0.065}$ $[8000 < Re < 24{,}000]$	–	0.850	1.196–3.042	1.107–2.586

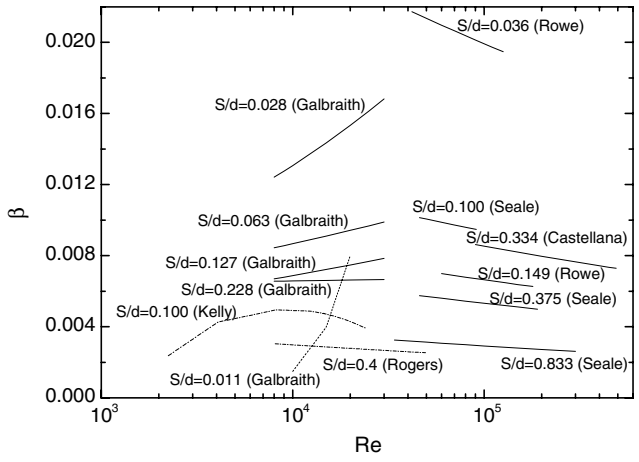

Fig. 2. Correlations of Table 2 for the mixing Stanton number.

the effects of a laminarization should be treated very carefully in the study of a turbulent mixing because the Schmidt number of about 1000, which is for the water experiment using a tracer technique, is far from the Prandtl numbers met in an actual design of an LMR or a PWR. It should be noted that the mass and heat transfer analogy is valid only if the Schmidt and the Prandtl numbers are of the same order of magnitude. For example, the water data of Galbraith and Knudsen for $S/d = 0.011$ seems to deviate considerably from the turbulent mixing rate for the Prandtl number of about unity. Generally speaking, the experiments with water using a tracer usually result in a lower turbulent mixing due to a significant laminarization than that obtained in a real design condition of a PWR.

In the results by Kelly and Todreas, the degree of laminarization predicted may be enhanced by the correction procedure for the error that may come from the entrance effect. It should be noted, as mentioned by Kelly and Todreas, that a small pressure imbalance could lead a remarkable redistribution of the flow split, thus, result in an inflation of mixing rate, especially in the experiments with water using a tracer technique. Therefore, the accuracy of this type of experiment for a small gap spacing and the range of the Reynolds number at which a laminarization appears are still controversial. From Fig. 2, we can induce two general trends of the turbulent mixing Stanton number. First, the effect of a laminarization appears up to a higher Reynolds number as the gap-to-diameter ratio decreases, which is consistent with our intuition if we adopt the view of Galbraith and Knudsen. Secondly, the turbulent mixing rate in square rod arrays is generally higher than that obtained in triangular rod arrays at the same gap-to-diameter ratio and the Reynolds number.

2.2. Turbulent mixing factor

The other type of mixing factor Y was first suggested by Ingesson and Hedberg [20]. Other researchers such as Rehme [8] and Moeller [21] have also adopted the same definition of a mixing factor in their studies. The turbulent mixing factor Y is defined in the following equation for a heat transfer through a gap between subchannels i and j per unit length by

$$q_{ij} = \rho c_p \bar{\varepsilon}_M S_{ij} Y \frac{T_i - T_j}{\delta_{ij}}, \tag{9}$$

where $\bar{\varepsilon}_M$ is the reference eddy viscosity obtained in a circular tube. The same heat transport is also described with the effective mean mixing velocity as follows:

$$q_{ij} = \rho c_p v_{\text{eff}} S_{ij} (T_i - T_j). \tag{10}$$

A comparison between Eqs. (9) and (10) yields a more direct expression of Y as follows:

$$Y = \frac{v_{\text{eff}}\delta_{ij}}{\bar{\varepsilon}_M}. \tag{11}$$

Therefore, a turbulent mixing through a gap between two neighboring subchannels per unit length is described as follows:

$$w'_{ij} = \frac{\rho S_{ij}\bar{\varepsilon}_M}{\delta_{ij}} Y. \tag{12}$$

Through intensive studies on the structure of the turbulence in the subchannels of rod bundles, Rehme [8] concluded that the natural mixing between the subchannels mainly results from the periodic flow pulsations and the secondary flow motion does not contribute significantly to the mixing process. He derived the following correlation based on a large number of experimental data and the investigation results from the early 1960s to 1990:

$$Y = \frac{0.7}{(S_{ij}/d)}. \tag{13}$$

Even though a considerable scattering of the data was found in the derivation of the correlation, the mixing factor developed by Rehme [8] is simple and effectively used for any gap geometry because the structure of turbulence due to periodic flow pulsations is incorporated well. Rehme described that the scattering of data is due to the geometrical tolerances of the test sections, the measuring techniques, and the disturbances of the flow fields by the probes and by the spacers.

If we examine the turbulent mixing factor Y defined by Eq. (9), it is found that this definition is not always applicable for a liquid having a low Prandtl number such as liquid metals whose eddy diffusivity of the momentum deviates considerably from the eddy diffusivity of the energy when the turbulent Peclet number is not so large as described by Kays [22]. In other words, when the turbulent Prandtl number defined by the ratio of the eddy diffusivity of momentum ε_M to the eddy diffusivity of energy ε_H is not unity, the relation of Eq. (9) is not valid any more. Only in the case of $\varepsilon_M/\varepsilon_H = 1$, the heat transfer due to a turbulent mixing through a gap can be described by

$$q_{ij} = \rho c_p \varepsilon_M S_{ij}\left(\frac{\partial T}{\partial n}\right)_S = \rho c_p \varepsilon_M S_{ij}\frac{T_i - T_j}{z_{ij,M}}. \tag{14}$$

When the turbulent Prandtl number is not unity, the exact relation of the heat transfer across the gap is described from the definition of ε_H as follows:

$$q_{ij} = \rho c_p \varepsilon_H S_{ij}\left(\frac{\partial T}{\partial n}\right)_S = \rho c_p \varepsilon_H S_{ij}\frac{T_i - T_j}{z_{ij,H}}. \tag{15}$$

By comparing Eq. (15) to Eq. (9), one obtains the mixing factor, Y described by

$$Y = \frac{\varepsilon_H}{\bar{\varepsilon}_M}\cdot\frac{\delta_{ij}}{z_{ij,H}}. \tag{16}$$

Zeggel and Monir [23] also used this definition of Y for the evaluation of a turbulent mixing rate with the VANTACY-II code. If we correlate the experimental results with this definition of Y for various fluids, especially when we include the results for liquid metals, the scattering of data is unavoidable even though other possible sources of a data scattering, such as the geometrical tolerances of the test sections, the measuring techniques, and the disturbances of the flow fields, are finely controlled. This is because the ratio of the effective eddy diffusivity of energy to the reference eddy viscosity changes a lot for different fluids and for different thermal-hydraulic conditions. Further, the ratio of effective mixing distance to the centroid distance is not conserved for different geometrical configurations, that is, for square arrays and for triangular arrays. It is notable that the transition from a laminar to a turbulent flow in the gap region occurs at different Reynolds numbers for square arrays and for triangular arrays at the same pitch-to-diameter ratio as commented on by Ramm [13].

In Table 3, the experimental conditions for various turbulent mixing experiments are summarized. The conditions for the experiments by Petrunik [18], Walton [24], and Kjellstrom [25] in Table 3 are obtained from the work of Kelly and Todreas [16]. It is noted that most data for the square rod arrays were obtained at a higher Reynolds number in a flow path with heated rods, therefore, the mixing factors were determined from the measured exit temperatures. On the contrary, most data for the triangular arrays were evaluated indirectly from the measured concentration of a tracer at a rather lower Reynolds number. It should be noted that it requires considerable effort to obtain reliable mixing data with a tracer because large entrance lengths are needed to obtain asymptotic values of mixing coefficients at low Reynolds numbers and high Prandtl numbers as mentioned by Ramm [13]. Kelly and Todreas [16] also reported that it was very difficult to remove the entrance effects and to exclude the effect of a diversion flow in the experiments using tracers.

In Fig. 3, all the experimental data of the turbulent mixing factor Y for both a square rod array and a triangular rod array, which is summarized in Table 3, is plotted against the gap-to-diameter ratio. Actually, most experimental data except the data by Moeller's [21] was given in the forms of β, St_g, or w'_{ij}/μ, which can be converted to Y or Y_H with the relation described in Table 1. In Fig. 3, it is easily found that the dependency of the mixing factor on the Reynolds number, Re, can not be excluded and a considerable scattering of the data exists. This scattering of the data could be due to the various reasons mentioned above. The first-hand data of Petrunik [18], Walton

Table 3
Experimental conditions and measurement techniques in the previous mixing studies

Experimenter	Channel type	Fluid	Pr	d (mm)	S/d	Re	Experimental technique	Heating type simulated
Rowe and Angle [9]	S-T	Water	1.0447	14.30	0.036 0.149	4.2×10^4–1.26×10^5 6.0×10^4–1.80×10^5	Exit enthalpy and code simulation	Electrical rod heating
Castellana [10]	S-S	Water	0.82–0.93	10.72	0.334	9.0×10^4–4.90×10^5	Exit enthalpy and code simulation	Electrical rod heating
Seale [11]	S-S	Air	0.702–0.709	50.00	0.100 0.375 0.833	4.6×10^4–9.10×10^4 4.6×10^4–1.90×10^5 3.4×10^4–3.00×10^5	Pitot-temperature probe for velocity and temperature distribution	Uniform duct wall heat flux
Singh and Pierre [19]	S-S	Water and air	$Sc \sim 1000$ ~ 1	21.34 20.83 19.81	0.018 0.043 0.102	1.3×10^3–3.80×10^4	Tracer and mixing or pressure balance	Plane source
Galbraith and Knudsen [17]	S-S	Water	$Sc \sim 1000$	25.40	0.011 0.028 0.063 0.127 0.228	8.0×10^3–3.00×10^4	Tracer and pressure balance	Plane source
Moeller [21]	S-S	Air	0.7078	157.5 157.5 157.5 157.5 157.5 157.5 139.0	0.007 0.018 0.036 0.072 0.100 0.148 0.223	$\sim 5.0 \times 10^4$	Hot wire and microphone	–
Kelly and Todreas [16]	T-T	Water	$Sc \sim 1000$	38.10	0.100	2.0×10^3–2.4×10^4	Tracer and pressure balance	Plane source
Walton [24]	T-T	Water Air	$Sc \sim 1000$ ~ 1	20.22	0.05	1.9×10^3–5.7×10^3 4.8×10^3–9.1×10^4	Tracer and pressure balance	Plane source
Petrunik [18]	T-T	Water	$Sc \sim 1000$	19.81	0.033 0.068 0.13	1.35×10^3–1.08×10^4 3.9×10^3–2.5×10^4 4.4×10^3–3.8×10^4	Tracer and mixing balance	Plane source
		Genetron	3.5		0.13	7.0×10^3–4.5×10^4	Temp. measurement	
Rogers and Tahir [14]	T-T	Air	~ 1	25.4	0.40	8.1×10^3–4.95×10^4	Tracer and pressure balance	Plane source
Roidt [29]	T-T	Air	~ 1	63.5	0.256	7.0×10^4	Tracer and calculated diversion cross plains	Point source
Kjellstrom [25]	T-T	Air	~ 1	156.5	0.217	1.5×10^5–3.6×10^5	Hot wire anemometer	–
Zukov [26]	T-T	Na NaK	0.0077 0.0237 0.0308 0.0300	14.0 12.0 24.7 15.8	0.150 0.130 0.214 0.320	8.60×10^3–3.70×10^4 3.80×10^3–1.70×10^4 1.10×10^4–4.10×10^4 1.60×10^4–5.00×10^4	Electro-magnetic device and micro-thermocouple	Central rod heating

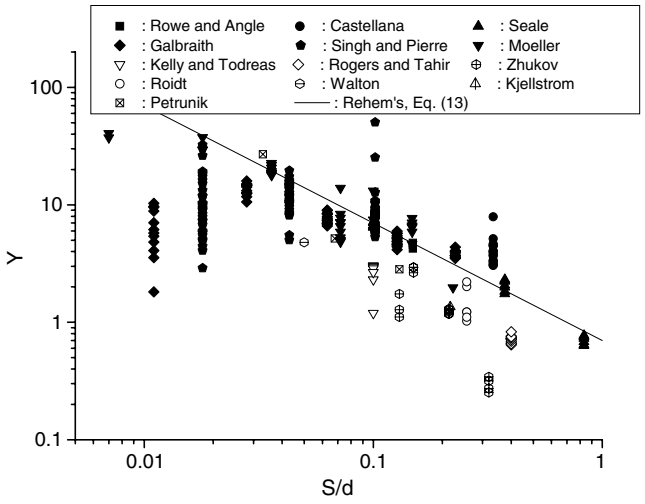

Fig. 3. Evaluated turbulent mixing factor with the definition of Y.

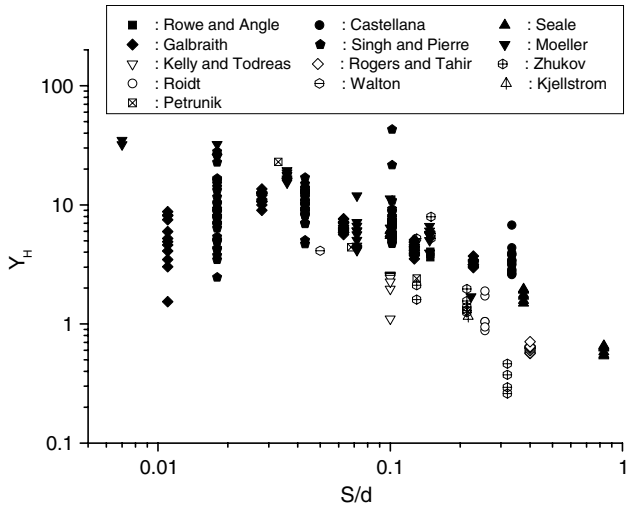

Fig. 4. Turbulent mixing data with the definition of Y_H.

[24], and Kjellstrom [25] was not available to the present authors, so it is cited from the study by Rehme [8].

3. Dominant parameter affecting the turbulent mixing rates

To treat the mixing data for a low Prandtl-number fluid such as a liquid metal consistently with the other mixing data obtained from the experiments with water or air, the mixing factor, Y_H defined by

$$q_{ij} = \rho c_p \bar{\varepsilon}_H S_{ij} Y_H \frac{T_i - T_j}{\delta_{ij}} \tag{17}$$

is suggested. In Eq. (17), $\bar{\varepsilon}_H$ is the reference eddy diffusivity of the energy obtained in a circular tube. The comparison between Eq. (17) to Eq. (10) gives

$$Y_H = \frac{v_{\text{eff}}\delta_{ij}}{\bar{\varepsilon}_H}. \tag{18}$$

Also, if Eqs. (15) and (17) are merged, it yields

$$Y_H = \frac{\varepsilon_H}{\bar{\varepsilon}_H} \cdot \frac{\delta_{ij}}{z_{ij,H}} = Y \cdot Pr_{\text{t}}. \tag{19}$$

Eq. (19) implies that the geometry of a flow path is a dominant parameter to determine a turbulent mixing in rod bundles when we evaluate a mixing with the mixing factors, Y or Y_H. In Fig. 4, the data of a new mixing factor Y_H for various experiments are summarized. The turbulent Prandtl numbers for the experiments are determined with the following correlation suggested by Kays [22]:

$$Pr_{\text{t}} = \frac{0.7}{Pe_{\text{t}}} + 0.85, \tag{20}$$

where Pe_{t} is the turbulent Peclet number defined by $(\varepsilon_M/v)Pr$. It is notable that the scattering of the liquid metal data by Zhukov [26] is reduced quite considerably when it is compared with Fig. 3. However, there still exists a quite large scattering of the data, especially at a lower S/d ratio, which suggests the independent geometrical parameter S/d is not a good correlating factor.

To get a better geometrical parameter which correlates the experimental data well, some mathematical manipulation is needed. If we combine Eqs. (3), (7), (11) and (18), a useful relation of the turbulent mixing factor is yielded as follows:

$$Y_H = \left(\frac{\delta_{ij}}{D_{\text{h}}}\right) \cdot \left(\frac{v}{\bar{\varepsilon}_H}\right) \cdot Re \cdot \beta \tag{21}$$

or

$$Y_H = \left(\frac{\delta_{ij}}{D_{\text{h}}}\right) \cdot \left(\frac{\bar{\varepsilon}_M}{v}\right)^{-1} \cdot Re \cdot \beta \cdot Pr_{\text{t}}. \tag{22}$$

The experimental data of a turbulent mixing obtained by various researchers are reevaluated into the form of Y_H and the dependency of various experimental turbulent mixing data on the geometrical parameter δ_{ij}/D_{h} is depicted in Fig. 5. When Fig. 5 is compared with Fig. 4, it is found that the parameter δ_{ij}/D_{h} correlates the experimental data better, especially the data obtained in a compact rod bundle, i.e., the data for a higher δ_{ij}/D_{h}. Therefore, it is estimated that the geometrical parameter δ_{ij}/D_{h} is a more dominant parameter than the gap-to-diameter ratio S/d which is frequently used in the existing correlations developed by previous researchers.

By the way, some data shown in Fig. 5 is not appropriate to describe a pure turbulent mixing because the effect of a laminarization is included at a lower S/d and a lower Re range. As mentioned previously, the degree of a turbulent mixing could also be distorted because of the pressure imbalance in the experiments with water using a tracer technique. The data obtained by Galbraith and Knudsen and by Kelly and Todreas seems to have a laminarization effect. The data reported by Petrunik, especially for a compact gap, is evaluated to include the pressure imbalance problem, therefore, the accuracy of this type of experiment may not be adequate for the test section of a smaller S/d. Evidently, the data by Singh and Pierre with water at a Reynolds number less than 1600 deviates considerably

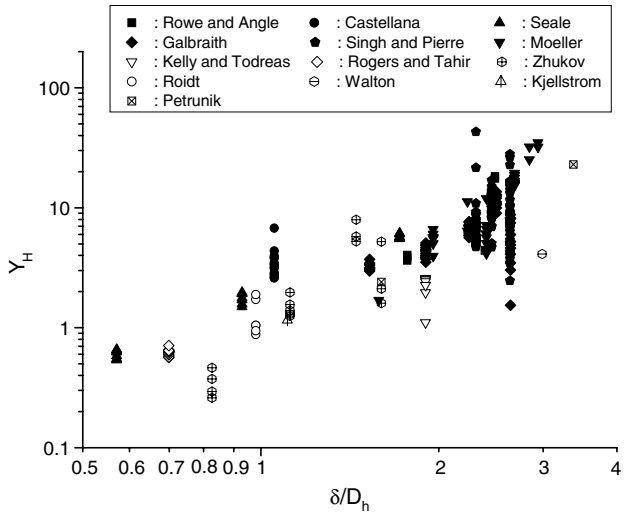

Fig. 5. Turbulent mixing factor Y_H with the independent geometrical parameter δ_{ij}/D_h.

from the group of the other mixing data, which suggests clearly the distortion by a pressure imbalance. It is also noted that the molecular diffusion plays an important role at this lower Re condition.

In Fig. 6, all the available experimental data, which is evaluated to have enough reliability, are summarized to obtain a useful correlation depending on the dominant geometrical parameter δ_{ij}/D_h. The selected data are the water mixing data determined by using the exit enthalpy measurement or the hot-wire technique. The air data determined with the tracer technique are included because the probability of a distortion due to the pressure imbalance is relatively low when air is used as a working fluid. The data shown in Fig. 6 is reduced into a correlation expressed as follows:

$$Y_H = 1.5615 \cdot \left(\frac{\delta_{ij}}{D_h}\right)^{2.013}. \tag{23}$$

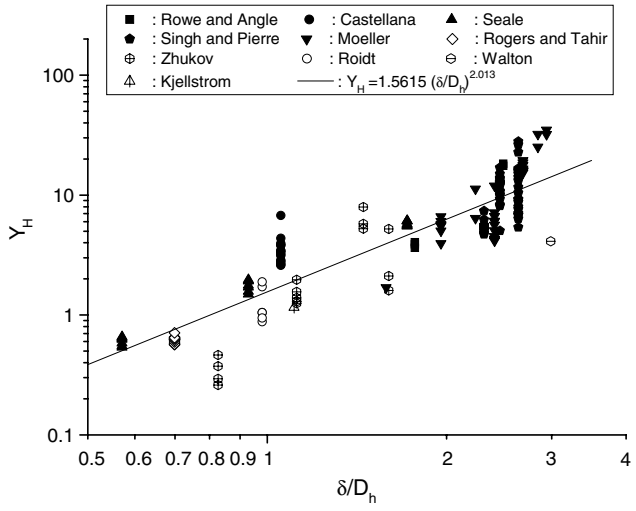

Fig. 6. Data fit for the meaningful turbulent mixing data in rod arrays.

The correlation of Eq. (23) is evaluated to be applicable for both square and triangular arrays. Even though the triangular data used in the derivation are generally lower than the data for the square array, the deviation is not so remarkable.

For the square rod arrays, it is possible to have general expressions of the eddy diffusivity and the turbulent mixing coefficient β, therefore, a simple relation for the turbulent mixing factor Y_H can be obtained. It is generally known that the eddy diffusivity is described with the Reynolds number and a friction factor as follows:

$$\varepsilon \propto v \cdot Re\sqrt{f/8}, \tag{24}$$

where f is the Darcy friction factor. The friction factor is known to be a function of the Reynolds number as follows:

$$f = a \cdot Re^b. \tag{25}$$

Therefore, the eddy diffusivity can be expressed as

$$\frac{\varepsilon}{v} = m \cdot Re^n. \tag{26}$$

In Table 1, the expressions of eddy diffusivity suggested by several researchers are summarized. Rowe and Angle [9] evaluated the turbulent mixing flow rate from the measured exit enthalpy and suggested that the eddy diffusivity of energy in square arrays is

$$\frac{\varepsilon_H}{v} = 0.0062 \cdot Re^{0.9}. \tag{27}$$

Kelly and Todreas [16] measured the Fanning friction factor in triangular rod arrays for $Re > 8000$ to obtain the expression of

$$f' = 0.0780 \cdot Re^{-0.228}, \tag{28}$$

which is similar to the Blasius equation. Based on this friction factor, Kelly and Todreas suggested a correlation of the eddy diffusivity of energy useful for $8000 < Re < 24{,}000$ as follows:

$$\frac{\varepsilon_H}{v} = 0.0045 \cdot Re^{0.89}. \tag{29}$$

Seale [11] also borrowed the friction factor measured in parallel plates by Hussain and Reynolds [27] and proposed a correlation of the eddy viscosity described in Table 1.

From the expression of the eddy diffusivity summarized in Table 1, it is found that the exponent n in Eq. (26) for the eddy diffusivity both in a circular tube and rod arrays is about 0.9. Therefore, the eddy viscosity and the kinematic viscosity have the following relation in a highly turbulent region:

$$\frac{\bar{\varepsilon}_M}{v} = K \cdot Re^{0.9}, \tag{30}$$

which can be used as a reference eddy viscosity to evaluate the turbulent mixing factor, Y_H with Eq. (22).

Kays [28] proposed an empirical equation for a friction factor in a circular tube applicable over the range of $3 \times 10^4 < Re < 10^6$ as follows:

$$f = 0.184 \cdot Re^{-0.2}. \tag{31}$$

As suggested by several previous researchers [8,20,21], we can evaluate the reference eddy viscosity expressed by

$$\frac{\bar{\varepsilon}_M}{\nu} = \frac{Re}{20}\sqrt{\frac{f}{8}}. \tag{32}$$

Combining Eqs. (31) and (32) yields a reference eddy viscosity for $3 \times 10^4 < Re < 10^6$ given by

$$\frac{\bar{\varepsilon}_M}{\nu} = 0.00758 \cdot Re^{0.9}, \tag{33}$$

which is nearly the same as the reference eddy viscosity used by Rehme [8].

A general expression on the turbulent mixing coefficient β in square rod arrays can be obtained directly from the experimental data. The experiments by Rowe and Angle [9], Castellana [10], and Seale [11] were performed at Reynolds numbers higher than 3.0×10^4 by using the exit temperature or enthalpy measurement in square rod arrays. In these experiments, the error for the turbulent mixing rate induced by the measurement technique itself is much less than the experiment using a tracer technique. The major error in this type of experiment would come from the entrance effect if the length of the test section is not enough. Even though there exists a considerable scattering for the turbulent mixing coefficient, all the researchers who measured the mixing coefficients at Reynolds number higher than 3.0×10^4 commonly summarized their experimental data into the form of

$$\beta = B \cdot Re^{-0.1}. \tag{34}$$

The value of B varies depending on the test section geometry as summarized in Table 3 and also depicted in Fig. 2.

With the previously determined eddy diffusivity of Eq. (30) and the turbulent mixing Stanton number of Eq. (34), Eq. (22) is converted to

$$Y_H^* = \frac{B}{K} \cdot \left(\frac{\delta_{ij}}{D_h}\right) \cdot Pr_t \tag{35}$$

The above equation implies that the turbulent mixing factor in a square array is nearly independent of the Reynolds number and that the geometrical factors are the most important parameters affecting a turbulent mixing at a highly turbulent condition. In Fig. 7, the data of the *Re*-independent turbulent mixing factor Y_H^* are plotted. These *Re*-independent mixing factors for square arrays are correlated with the following equation:

$$Y_H^* = 2.037 \cdot \left(\frac{\delta_{ij}}{D_h}\right)^{2.071}. \tag{36}$$

It should be noted that the derived correlation of Eq. (36) is applicable in the range of

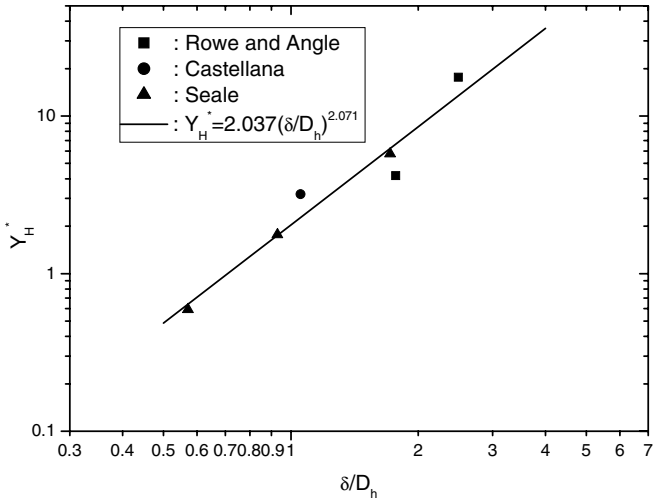

Fig. 7. *Re*-independent turbulent mixing factor for square arrays.

$$3.0 \times 10^4 \leqslant Re \leqslant 1.0 \times 10^6 \quad \text{and} \quad 0.57 \leqslant \frac{\delta_{ij}}{D_h} \leqslant 2.94.$$

4. Conclusions

Through a survey of the existing experimental data it is found that the turbulent mixing factor Y defined by Eqs. (9) and (16) is appropriate only for a high Prandtl number fluid when the turbulent Peclet number is also high. A new definition of mixing factor Y_H was introduced to correlate all the mixing data consistently including the data for the low Prandtl number fluids such as liquid metals. With this definition of a mixing factor it is also found that the geometrical parameter δ_{ij}/D_h is a dominant factor affecting a turbulent mixing, which correlates the reliable experimental data better than the gap-to-diameter ratio S/d. A useful correlation of Eq. (23) for a turbulent mixing in rod arrays was obtained as a function of only δ_{ij}/D_h. The correlation is applicable for both square and triangular arrays with a reasonable accuracy, which implies that the geometrical parameter δ_{ij}/D_h represents the characteristic mixing length for both square and triangular arrays quite well. The correlation predicts a reasonable mixing at a higher δ_{ij}/D_h or at a lower S/d ratio, which is the most improved feature of the correlation when compared with the existing ones. The general expressions for the eddy diffusivity and the turbulent mixing coefficient β for square rod arrays was obtained to derive a Reynolds number-independent mixing correlation of Eq. (36), which is applicable for square array at highly turbulent conditions. The developed correlations have to be validated further with more experimental data for liquid metals.

Acknowledgement

This work has been performed under the Long-term Nuclear R&D Programs supported by Ministry of Science and Technology (MOST), Korea.

References

[1] K.S. Ha, H.Y. Jeong, W.P. Chang, Y.M. Kwon, Y.B. Lee, Wire-wrap models for subchannel blockage analysis, J. Korean Nucl. Soc. 36 (2) (2004) 165.

[2] H. Ninokata, A. Efthimiadis, N.E. Todreas, Distributed resistance modeling of wire-wrapped rod bundles, Nucl. Eng. Des. 104 (1987) 93.

[3] S.K. Cheng, N.E. Todreas, Hydrodynamic models and correlations for bare and wire-wrapped hexagonal rod bundles – bundle friction factors, subchannel friction factors and mixing parameters, Nucl. Eng. Des. 92 (1986) 227.

[4] E.H. Novendstern, Turbulent flow pressure drop model for fuel rod assemblies utilizing a helical wire-wrap spacer system, Nucl. Eng. Des. 22 (1972) 19.

[5] C.W. Stewart, C.L. Wheeler, R.J. Cena, C.A. McMonagle, J.M. Cuta, D.S. Trent, COBRA-IV: The model and the method, BNWL-2214, Pacific Northwest Laboratories, 1977.

[6] H.Y. Jeong, K.S. Ha, W.P. Chang, Y.M. Kwon, Y.B. Lee, Modeling of flow blockage in a liquid metal-cooled reactor subassembly with a subchannel analysis code, Nuclear Technol. 149 (2005) 71.

[7] M.R. Yeung, L. Wolf, Evaluation of conduction mixing lengths for subchannel analysis of finite LMFBR bundles, Nucl. Eng. Des. 62 (1980) 371.

[8] K. Rehme, The structure of turbulence in rod bundles and the implications on natural mixing between the subchannels, Int. J. Heat Mass Transfer 35 (1992) 567.

[9] D.S. Rowe, C.W. Angle, Crossflow mixing between parallel flow channels during boiling, Part II: Measurement of flow and enthalpy in two parallel channels, BNWL-371 PT2, Pacific Northwest Laboratory, 1967.

[10] F.S. Castellana, W.T. Adams, J.E. Casterline, Single-phase subchannel mixing in a simulated nuclear fuel assembly, Nucl. Eng. Des. 26 (1974) 242.

[11] W.J. Seale, Turbulent diffusion of heat between connected flow passages, Part 1: Outline of problem and experimental investigation, Nucl. Eng. Des. 54 (1979) 183.

[12] S.-K. Cheng, N.F. Todreas, Constitutive correlations for wire-wrapped subchannel analysis under forced and mixed convection conditions, DOE/ET/37240-108TR, MIT, Cambridge, Massachusetts, 1984.

[13] H. Ramm, K. Johannsen, N.E. Todreas, Single phase transport within bare rod arrays at laminar, transition and turbulent flow conditions, Nucl. Eng. Des. 30 (1974) 186.

[14] J.T. Rogers, A.E.E. Tahir, Turbulent interchange mixing in rod bundles and the role of secondary flows, ASME Paper 75-HT-31, 1975.

[15] X. Cheng, N.I. Tak, CFD analysis of thermal-hydraulic behavior of heavy liquid metals in sub-channels, Nucl. Eng. Des. 236 (2006) 1874.

[16] J.M. Kelly, N.E. Todreas, Turbulent interchange in triangular array bare rod bundles, COO-2245-45TR, MIT, Cambridge, Massachusetts, 1977.

[17] K.P. Galbraith, J.G. Knudsen, Turbulent mixing between adjacent channels for single-phase flow in a simulated rod bundle, in: 12th Natn. Heat Transfer Conf., Tulsa, Oklahoma, AIChE Symposium Series, No. 118, vol. 68, 1971, pp. 90–100.

[18] K. Petrunik, Turbulent mixing measurement for single phase air, single phase water, and two phase air–water flows in adjacent rectangular subchannels, M.A.Sc. Thesis, University of Windsor, Ont. 1968.

[19] K. Singh, C.C.St. Pierre, Single phase turbulent mixing in simulated rod bundle geometries, Trans. CSME 1 (2) (1972) 73.

[20] L. Ingesson, S. Hedberg, Heat transfer between subchannels in a rod bundle, Heat Transfer 1970, Paris, vol. III, FC 7.11, Elsevier, Amsterdam, 1970.

[21] S.V. Moeller, Single-phase turbulent mixing in rod bundles, Exp. Therm. Fluid Sci. 5 (1992) 26.

[22] W.M. Kays, Turblent Prandtl number—Where are we? J. Heat Transfer 116 (1994) 284.

[23] W. Zeggel, C. Monir, Prediction of natural mixing in tightly packed 7-rod-bundles ($p/d = 1.10$), in: Proc. Fourth Int. Topical Meeting on Nuclear Reactor Thermal-Hydraulics (NURETH-4), vol. 2, Karlsruhe, Germany, October 10–13, 1989, p. 1294.

[24] F.B. Walton, Turbulent mixing measurements for single phase air, single phase water, and two phase air–water flows in adjacent triangular subchannels, M.S. Thesis, University of Windsor, Ont., 1969.

[25] B. Kjellstrom, Transport process in turbulent channel flow, Final Report AE-RL-1344, Aktiebolaget Atomenergi, Studsvik, 1971.

[26] A.V. Zhukov, N.A. Kotovskii, L.K. Kudryavtseva, N.M. Matyukhin, E.Ya. Sviridenko, A.P. Sorokin, P.A. Ushakov, Yu.S. Yur'ev, Comecon-Symposium Teplofizika i gidrodinamika aktivnoi zony i parogeneratorov dlya bystrykh reaktorov, Marianske Lazne, CSSR, April 4–8, 1978, CKAE, Prag 1978, vol. 1, Paper ML 78/09, 114–127 (in Russian); German translation KfK-tr-657, Kernforschungszentrum Karlsruhe, F.R.G., 1980.

[27] A.K.M.F. Hussain, W.C. Reynolds, Measurements in fully developed turbulent channel flow, J. Fluids Eng. (Dec.) (1975) 568.

[28] W.M. Kays, H.C. Perkins, Forced convection, internal flow in ducts, Handbook of Heat Transfer Fundamentals, second ed., McGraw-Hill, Inc., 1985, p. 7-5.

[29] M. Roidt, M.J. Pechersky, R.A. Markley, B.J. Vegter, Determination of turbulent exchange coefficients in a rod bundle, J. Heat Transfer (May) (1974) 172.

[30] J.T. Rogers, R.G. Rosehart, Mixing by turbulent interchange in fuel bundles. Correlations and influences, ASME Paper 72-HT-53, AIChE-ASME Heat Transfer Conference, Denver, Colorado, August 6–9, 1972.